

Studies of the Relativistic Electron Source and Related Phenomena in Petawatt Laser Matter Interactions

*M. H. Key, E. M. Campbell, T. E. Cowan, S. P. Hatchett,
E. A. Henry, J. A. Koch, A. B. Langdon, B. F. Lasinski, R.
W. Lee, A. MacKinnon, A. A. Offenberger, D. M.
Pennington, M. D. Perry, T. J. Phillips, M. Roth, T. C.
Sangster, M. S. Singh, R. Snavely, M. A. Stoyer, S. C.
Wilks, and K. Yasuike*

U.S. Department of Energy

Lawrence
Livermore
National
Laboratory

This article was submitted First International Conference on Inertial
Fusion Science and Applications, Bordeaux, France, September 12-
17, 1999

September 27, 1999

DISCLAIMER

This document was prepared as an account of work sponsored by an agency of the United States Government. Neither the United States Government nor the University of California nor any of their employees, makes any warranty, express or implied, or assumes any legal liability or responsibility for the accuracy, completeness, or usefulness of any information, apparatus, product, or process disclosed, or represents that its use would not infringe privately owned rights. Reference herein to any specific commercial product, process, or service by trade name, trademark, manufacturer, or otherwise, does not necessarily constitute or imply its endorsement, recommendation, or favoring by the United States Government or the University of California. The views and opinions of authors expressed herein do not necessarily state or reflect those of the United States Government or the University of California, and shall not be used for advertising or product endorsement purposes.

This is a preprint of a paper intended for publication in a journal or proceedings. Since changes may be made before publication, this preprint is made available with the understanding that it will not be cited or reproduced without the permission of the author.

This report has been reproduced
directly from the best available copy.

Available to DOE and DOE contractors from the
Office of Scientific and Technical Information
P.O. Box 62, Oak Ridge, TN 37831
Prices available from (423) 576-8401
<http://apollo.osti.gov/bridge/>

Available to the public from the
National Technical Information Service
U.S. Department of Commerce
5285 Port Royal Rd.,
Springfield, VA 22161
<http://www.ntis.gov/>

OR

Lawrence Livermore National Laboratory
Technical Information Department's Digital Library
<http://www.llnl.gov/tid/Library.html>

Studies of the Relativistic Electron Source and Related Phenomena in Petawatt Laser Matter Interactions

M. H. Key, E. M. Campbell, T. E. Cowan, S. P. Hatchett, E. A. Henry, J. A. Koch, A. B. Langdon, B. F. Lasinski, R. W. Lee, A MacKinnon , A. A. Offenberger¹, D.M. Pennington, M. D. Perry, T. J. Phillips, M Roth² , T. C. Sangster, M. S. Singh, R. Snavely, M. A. Stoyer, S. C. Wilks K Yasuike³.

Lawrence Livermore National Laboratory , POBox. 808, Livermore Ca 94550, USA.

¹Visiting from University of Alberta, Edmonton, Alberta, T6G 2G7, Canada.

²Visiting from GSI Laboratory, Darmstadt, Germany.

The interaction of laser radiation with solid targets at 1 petawatt power and intensity up to $3 \times 10^{20} \text{ Wcm}^{-2}$ has been studied with emphasis on relativistic electrons and high energy ions . Secondary effects including Bremsstrahlung radiation, nuclear interactions and heating have been characterized. A collimated beam of protons with up to 55 MeV energy is emitted normal to the rear surface of thin targets and its characteristics and origin are discussed The significance of the data for radiography , fast ignition and proton beam applications is summarized .

1.Introduction

The petawatt (PW) laser system at LLNL¹ generates 1PW pulses of 500 fs duration using chirped pulse amplification(CPA) in one beam line of the 10 beam Nova facility . A 37 actuator Deformable mirror installed in May 1998 controlled the wavefront and raised the peak intensity with f/3 focussing to $3 \times 10^{20} \text{ Wcm}^{-2}$. About 30% of the pulse power was within the first minimum of the focal spot which had an 8 to 9 μm f.w.h.m. Amplified spontaneous emission in a 4 ns period before the main pulse had about 10^{-4} of the main pulse energy and there was a 10^{-4} leakage pre-pulse 2 ns before the main pulse. These pre-pulses generated a preformed plasma which was measured by sub picosecond pulse optical interferometry to have an on axis electron density of $3 \times 10^{19} \text{ cm}^{-3}$ in a plane 70 μm from a planar CH target with an approximately exponential fall to lower densities having a scale length of 40 μm . The interaction of the focused main pulse with the pre-formed plasma and processes in the underlying planar solid target were studied to determine the characteristics of the relativistic electron source and related phenomena².

2.Electrons

Relativistic self focussing in the preformed plasma³ is an important factor in the interaction evidenced in our work by an invariant x-ray emission spot of about 20 micron diameter (with suggestions of a substructure of multiple spots due to relativistic filaments) as the focal plane was displaced as much as 300 micron in front of the target⁴. We have previously reported on measurements of the energy spectrum of electrons

emitted into vacuum from the rear surface of 1 mm thick Au targets^{2,4,5}. Data show energies up to 100 MeV with a quasi exponential slope temperature of 5 to 10 MeV and there indications of non thermal peaks in the spectrum which are discussed in the present proceedings in another paper⁶. Of particular interest is the observation of positron emission from 1mm thick Au targets which can be associated primarily with pair production in the absorption of Bremsstrahlung photons. Thinner Au targets show an excess of positrons over the level due to absorption of photons⁶ and this may indicate the first evidence of a laboratory electron- positron plasma sustained by collisional production of positrons⁷.

Radiochromic (RC) film in a multilayer conical assembly recording over the forward hemisphere via several different thickness of Ta (see figure 2), revealed the angular pattern of relativistic electron emission for typically 100 micron thick Au and CH targets irradiated at 0 or 45° incidence, as a diffuse background of wide angular range shown in figure 1. The approximate source temperature and energy content of the electron emission were determined by quantitative analysis. Typical results were 1 to 2 J of electrons and a temperature of 3 to 4 MeV. These numbers are consistent with the magnetic spectrometer data discussed previously. The total emitted energy corresponds to the maximum charge which can leave the target before the Coulomb potential traps the major fraction of the electrons. The angular pattern has one (and sometimes more than one) broad peak in random directions in the forward hemisphere. A similar angular pattern observed in emitted Bremsstrahlung x-rays is described later.

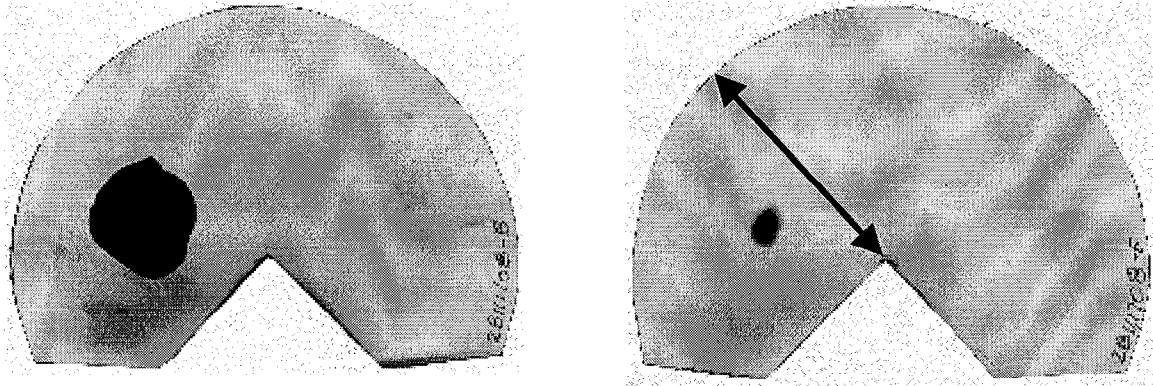


Figure 1 . Radiochromic film images from conical detector; left via 200 μ m Ta (>14MeV) and right via 600 μ m Ta (>26 MeV) . Arrow indicates 90° angle range (see figure2) . Target was 1 mm square 125 mm thick Au foil irradiated at 45° P polarized incidence .

3. Protons

A very reproducible collimated intense beam seen in figure 1 was emitted perpendicular to the rear surface of the target for both normal and 45° incidence. It

narrows sharply in angle as the Ta layer thickness is increased. We have studied this beam and have shown it to be due to proton emission with energies up to 60 MeV and total energy content as high as 30 J (the latter for normal incidence on 100 micron thick CH) . After an initial misinterpretation as an electron beam shortly after the beam was first observed ⁴ the proton identity of the beam was suggested to us by analysis of etched tracks in filtered CR39 plastic which gave evidence of > 30 MeV protons . Subsequent re-analysis of the RC film images assuming the beam to be protons , gave a plausible energy content of 10J and source temperature of about 4 MeV for the conditions of figure 1 .Unambiguous confirmation was obtained by recording the energy spectrum of the protons on the axis of the beam and at 45 ° off axis with the magnetic spectrometer ³ . A sharp cut off at high energy reaching 60 MeV on axis and 15 MeV at 45° was observed.

Specific attention was directed to whether the beam was normal to the front or the rear surface using the CH wedge target shown in figure 2. Very clear evidence was obtained that the emission was normal to the rear surface because two separate proton beams were observed corresponding to the major and minor “rear” surfaces of the 30° wedge. It is also interesting to note that RC images via the thinnest filters (25 µm Al) recording protons with energy > 4MeV showed a sheet of emission in the horizontal plane ⁴which we now attribute to proton emission from the vertical edges of the 1 mm square targets. With cones of radiochromic film placed both behind and (with a central hole for the laser beam)in front of a target irradiated at 45° there was no corresponding forward proton beam . Protons above the 4 MeV threshold energy for detection integrated over the forward hemisphere, had less than 5% of the energy recorded in the proton beam from the rear surface .

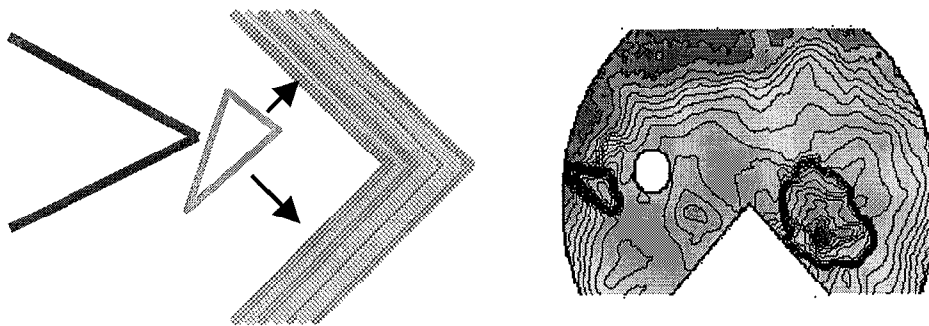


Figure 2. Left: conical detector with multiple layers of Ta and RC film covering the forward hemisphere for a CH wedge target .Right: contour intensity map of RC film image via 200 micron Ta (protons > 14 MeV) . The image shows two proton beams , the larger from the major face and the smaller from the minor face of the wedge as indicated by the arrows .

Further direct evidence that the beam is due to protons was obtained from a multilayer detector consisting of 250 μm Ti, 1.2 mm Be and 250 μm RC film (with several repeats). The yield of the nuclear process, $\text{Ti}^{48}(\text{p},\text{n})\text{V}^{48}$ was measured from the characteristic gamma emission of the activated V^{48} nuclei. These data when fitted to modelling, showed a detected proton energy $>40\text{MeV}$, a slope temperature of 6 MeV and assuming a Boltzman distribution, a total of 3×10^{13} protons or 30J of energy which was 7% of the laser energy incident on the target.

Clear confirmation that the RC film images show a proton beam was obtained from autoradiography images of activation in the Ti foils as seen in figure 3 which shows the correspondence of RC and autoradiography images recorded in adjacent layers of the detector on a single shot. A further diagnostic was the observation of 3×10^{10} neutrons in an Ag activation neutron detector. This yield was attributed to several neutron producing channels of proton interaction with Be nuclei.

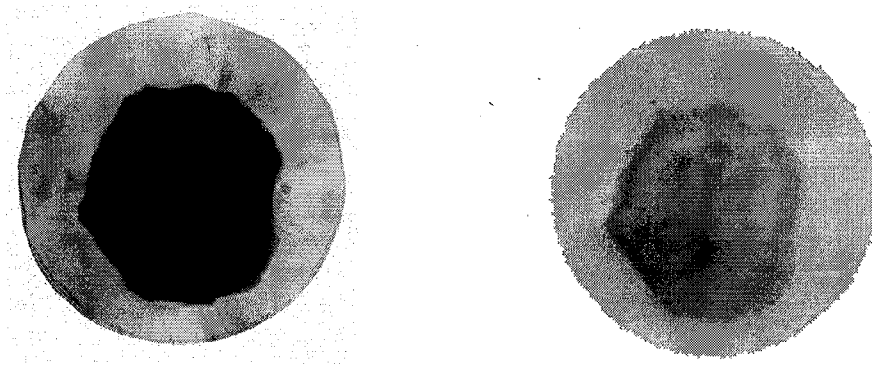


Figure 3 . Left radio-chromic film image and right corresponding autoradiography image of a Ti foil for 100 micron CH target at normal incidence .

We are currently analyzing and modelling the mechanism for the proton beam generation. There are essentially two main possibilities, which are discussed in the literature. One is forward ion acceleration by ponderomotive pressure in the laser focal spot on the front surface of the target⁸ and the other is electrostatic acceleration perpendicular to the surfaces of the target through hot electron pressure and double layer formation⁹.

We have rejected the first process because of the clear evidence that the protons are emitted perpendicular to the rear surface of the target. The evidence of proton emission from the edges of the target also supports a model of emission over an extended area much larger than the focal spot. The fact that protons are detected from Au targets is understood as emission from a monolayer of adsorbed molecules containing hydrogen. This could not come from the front surface focal region of our targets because of the pre-pulse induced blow off such monolayers into preformed plasma. Moreover an area of

the order of 1 mm^2 is needed to supply the observed number of protons from a mono layer.

We believe that the previously much studied process of fast ion generation by hot electrons⁹ adapted for very short pulse duration and for contrasting very short and long density scale lengths of the plasma on the front and back of the target, can explain our data.

Figure 4 illustrates how (via solution of Poisson's equation and applying Boltzman statistics) a suddenly created hot electron density in a pre-existing density gradient will exclude cold electrons at ion densities lower than the hot electron density, and set up a constant E field accelerating ions in the plasma. An ion charge sheet forms at the exclusion boundary and a Debye sheath at lower density where the scale length of the ion density profile matches the hot electron Debye length. The magnitude of the E field for a hot electron temperature T_h is given by $E = T_h / e L_i$ scaling inversely with the density scale length L_i .¹⁰ This shows that there will be much stronger acceleration at the sharp density interface on the back of the target and it results in a rate of energy transfer to ions, which is initially much greater at the rear surface. If the hot electrons dissipate their energy rapidly the result will be a larger energy transfer to ions at the back surface .

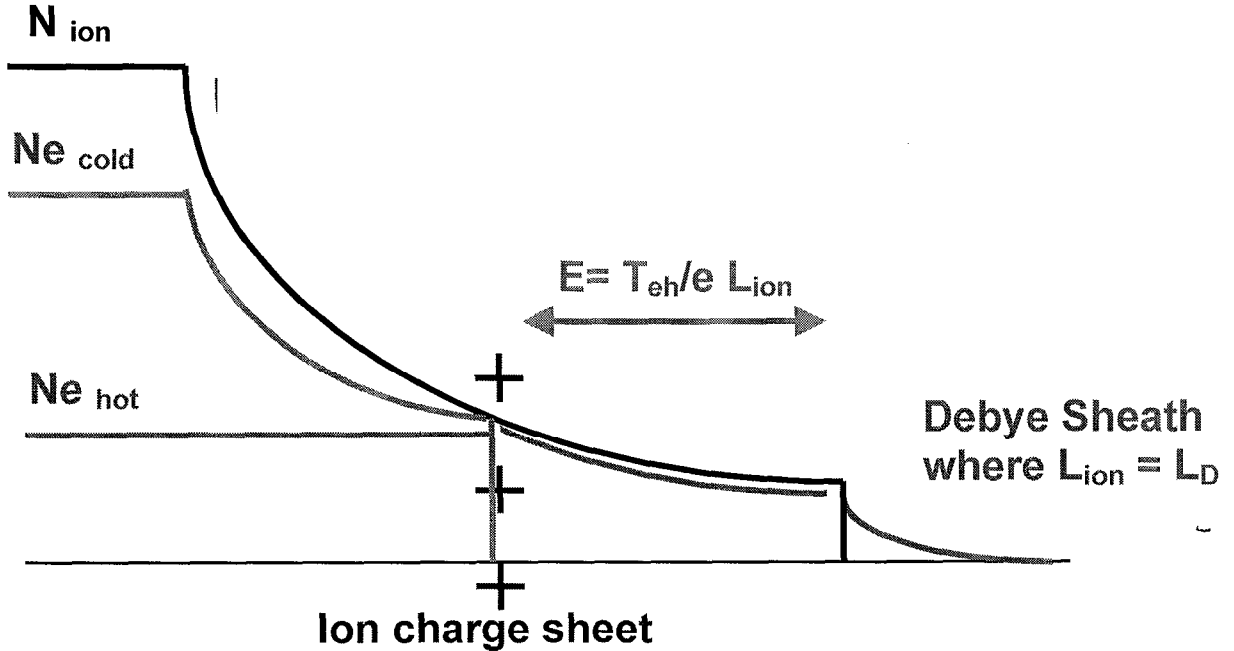


Figure 4

We have used ID PIC modeling to illustrate this process .Energy spectra of protons are computed at times up to 480 ps for a plasma initially at 10 times critical density with an electron temperature of 500 keV . The energy spectra show a high energy cut off at 3.7 MeV for a $0.05 \mu\text{m}$ linear density ramp and 1.6 MeV for a $14 \mu\text{m}$ linear ramp¹⁰.

Proton beams of the high energy, power and collimation observed could be of interest for numerous applications. More work is needed to characterise the emittance which will determine the focusability of the beam and its usefulness, for example, in replacing the front end of large accelerators or as an ignitor in fast ignition⁶.

4.x-rays

We have investigated the use of the relativistic electron source to produce intense hard x-rays for dynamic radiography¹¹. We used 1 mm thick Au targets as optimized Bremsstrahlung converters and studied their x-ray emission. The spectrum was determined in absolute units from TLD detectors with a range of filters (up to 2 cm thick Ta) which gave spectral data² in the range from about 0.1 to 5 MeV. At higher photon energies from 15 MeV to 60 MeV nuclear activation of Au via (γ, xn) processes with x up to 6, whose cross sections are shown in figure 5 gave spectra such as shown in figure 5. The solid line is from a model using MonteCarlo simulation with an electron source having an energy spectrum similar to that recorded with the magnetic spectrometer.

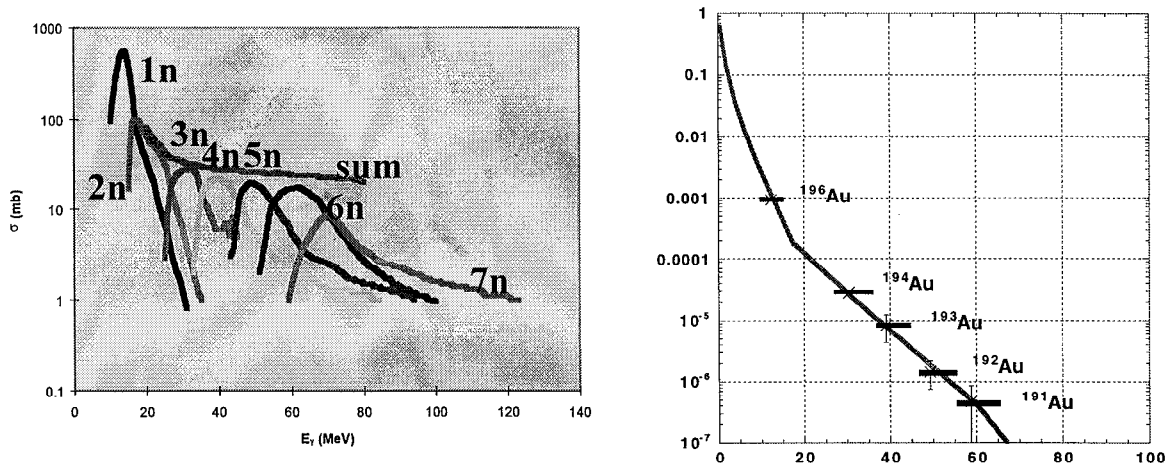


Figure 5 Left : (γ, xn) photo-neutron cross sections . Right: x-ray spectrum deduced from nuclear activation .Units are Photons/MeV / 7×10^{13} versus photon energy in MeV

The angular pattern of photon emission at around 15 MeV was determined from a hemisphere array of 31 Au discs. There was a reproducible quasi Gaussian peak of $\pm 50^\circ$ angle whose direction was essentially random for angles up to 45° off axis. A similar finer resolution hemisphere array of 150 TLD detectors with a flat response to x-ray energy at >0.5 MeV showed angular peaks in the same direction as the nuclear activation but with a broader angular range falling to half intensity at $\pm 90^\circ$. This detection system gave the hemisphere integrated x-ray yield which had significant shot to shot fluctuation as shown in figure 6. The data average to 11J of x-rays >0.5 MeV or 2.9%

conversion of incident laser energy. The hemisphere averaged rad level at 1m was about 0.5 and the peak was typically 2x higher. The highest recorded rad level at 1m was 2. The intensity of the source was sufficient to record contact radiographs via up to 15 cm Pb and to give 100 micron resolved images of a 10 cm test object with a complex structure having areal density up to 35 gcm^{-2} .

Monte Carlo modeling with different assumptions about the energy spectrum of the electrons was used to estimate the conversion of laser energy to electrons. The dependence of the conclusion on the assumed form of the energy spectrum was fairly weak and for the most plausible model which best matched the spectrum of the x-rays, this analysis indicated 40 to 50% conversion to relativistic electrons.

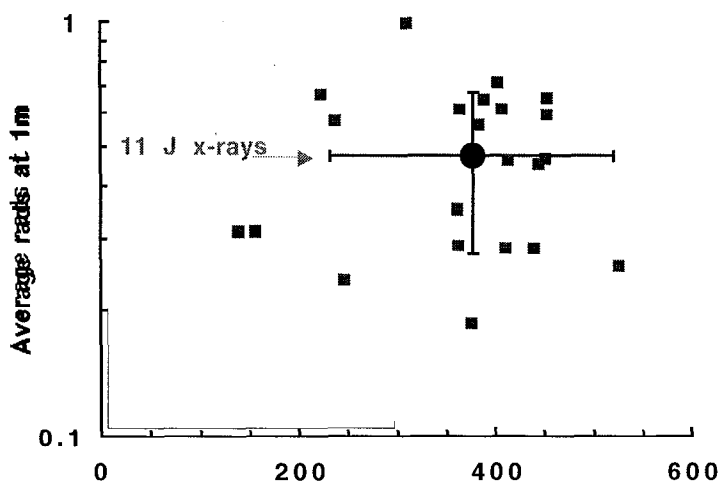


Figure 6. X-ray yield versus laser energy in J – average and individual shots .

The main issue for the application to MeV radiography is the wide beam angle of the x-rays which greatly reduced the rad level relative to that which would be obtained with similar conversion efficiency into a well collimated beam of electrons

5. Electron energy transport and heating by electrons

In the context of fast ignition¹², a crucial problem is the efficiency of energy transfer from a short pulse igniter beam to the ignition spark via the surrounding plasma atmosphere. The problem includes penetration of the beam to the critical density and transport of energy by electrons at densities much above the critical density .

We have examined the latter by seeking evidence of the heating effect of the electrons in solid targets⁴. Evidence of temperatures in the range 0.5 to 1keV was obtained⁴ from observation of a narrow DD thermonuclear fusion peak superimposed on

an intense broad background from γ, n and p, n processes, in neutron energy spectra. Data were recorded from targets of CD_2 with a front layer of CH or Cu.

Further evidence was obtained from x-ray spectra of Al emission from sensor layers buried up to 20 μm deep in CH targets¹³. Temperatures of about 300eV and density of 0.6 g/cc were recorded most recently¹⁴. Of particular interest were pinhole camera images of the x-rays from the Al which showed an annular pattern of heating with an 80 μm diameter. Images from the rear side of targets having Al layers up to 200 μm from the front surface and 5 micron below the rear surface, showed a similar annulus up to 100 micron inside the solid target¹⁴. Some emission was observed at 200 μm depth. These data strongly suggest heating in a collimated pattern as predicted by recent theoretical modelling of magnetically guided energy flow¹⁵. The annular pattern remains unexplained however and is the subject of further study.

6.Summary

In summary PW lasers open up new fields of scientific study. They offer efficient conversion to relativistic electrons which may exceed 40% Conversion to MeV x-rays reaches 3% but in a very wide angle beam. An intense collimated beam of energetic protons carrying up to 7% of the energy may open up new classes of applications. Evidence of collimated electron energy transport is encouraging for fast ignition but needs further study to understand its annular pattern.

Work performed under the auspices of the U.S. Department of Energy by the Lawrence Livermore National Laboratory under Contract No. W-7405-ENG-48.

7.References

-
- ¹ M Perry et al. Opt. Lett. 24, 160 (1999)
 - ² M H Key et al. Phys Plasmas. 5, 1966, (1998)
 - ³ A Pukhov, J Meyer ter Vehn, Phys. Rev. Lett. 76, 3975 (1996)
 - ⁴ M H Key et al. Proc 17th IAEA Fusion Energy Conf. (In press).
 - ⁵ T E Cowan et al. Lasers and Particle beams, (in press)
 - ⁶ M Roth et al. ibid.
 - ⁷ E P Liang, S C Wilks, M Tabak, Phys. Rev. Lett. 81, 4887 (1998)
 - ⁸ E Lefebvre, C Toupin, G Bonnaud ibid.
 - ⁹ Y Kishimoto K Mima, T Watanabe, K Nishikawa, Phys. Fluids 26, 2308 (1983) and references therein
 - ¹⁰ S Hatchett, S Wilks et al. (to be published)
 - ¹¹ M D Perry et al. Rev Sci Instr. 70, 266 (1999)
 - ¹² M Tabak et al Phys. Plasmas 1, 1626, (1994)
 - ¹³ J A Koch et al. Lasers and Particle Beams, 16, 225 (1998)
 - ¹⁴ J A Koch et al. ibid.
 - ¹⁵ J R Davies, A R Bell, M G Haines S Guerin, Phys Rev. E. 56, 7193 (1997)